Reinforcement of single-walled carbon nanotube bundles by intertube bridging

A. KIS[1], G. CSÁNYI[2], J.-P. SALVETAT[3], THIEN-NGA LEE[1], E. COUTEAU[1], A. J. KULIK[1], W. BENOIT[1], J. BRUGGER[4] AND L. FORRÓ[1]

[1]Institute of Physics of Complex Matter, Ecole Polytechnique Fédérale de Lausanne (EPFL), CH-1015 Lausanne, Switzerland
[2]Cavendish Laboratory, University of Cambridge, Cambridge CB3 0HE, UK
[3]Centre de Rechereche sur la matière devisée (CRMD), Centre National de la Recherche Scientifique (CNRS), F-45071 Orleans, France
[4]Institute of Microelectronics and Microsystems, EPFL, CH-1015 Lausanne, Switzerland
*e-mail: laszlo.forro@epfl.ch

Published online: 15 February 2004; doi:10.1038/nmat1076

During their production, single-walled carbon nanotubes form bundles. Owing to the weak van der Waals interaction that holds them together in the bundle, the tubes can easily slide on each other, resulting in a shear modulus comparable to that of graphite. This low shear modulus is also a major obstacle in the fabrication of macroscopic fibres composed of carbon nanotubes. Here, we have introduced stable links between neighbouring carbon nanotubes within bundles, using moderate electron-beam irradiation inside a transmission electron microscope. Concurrent measurements of the mechanical properties using an atomic force microscope show a 30-fold increase of the bending modulus, due to the formation of stable crosslinks that effectively eliminate sliding between the nanotubes. Crosslinks were modelled using first-principles calculations, showing that interstitial carbon atoms formed during irradiation in addition to carboxyl groups, can independently lead to bridge formation between neighbouring nanotubes.

Since their discovery, carbon nanotubes[1] have attracted the attention of many scientists and engineers worldwide, partly because of their exceptionally high Young's modulus. Initial measurements of the Young's modulus of carbon nanotubes have confirmed the theoretical expectation close to 1 TPa (10^{12} Pa), similar to the in-plane modulus of graphite[2,3]. However, single-walled carbon nanotubes (SWNT) often aggregate into bundles (ropes) of weakly interacting tubes that can easily slide on each other[2]. These bundles can contain up to several hundred SWNTs arranged in a hexagonal lattice[4]. The bending modulus of carbon nanotube bundles, which for a homogeneous bar corresponds to the Young's modulus, strongly decreases with the diameter of ropes (Fig. 1). The main cause for this apparent flaw is the weakness of the van der Waals force that binds the tubes together. Owing to weak intertube forces, thick ropes behave as loose bundles of individual tubes that can easily slide past each other, rather than as a thick bar. The same phenomenon of intertube sliding is encountered in the fabrication of macroscopic structures composed entirely of carbon nanotubes: ribbons and fibres[5,6], as well as centimetre-long strands[7]. With the Young's modulus of 80 GPa in the case of fibres[6] and 77 GPa for the strands[7], these remarkable structures still don't take full advantage of the superior mechanical properties of carbon nanotubes. Introducing stable connections between nanotubes, without significantly degrading their Young's modulus in the process, would bring their application closer to reality.

Carbon nanostructures have shown to be very sensitive to irradiation[8]. This sensitivity can be exploited for controllable modifications of their structural properties, as far as turning[9] sp^2-hybridized carbon into sp^3, or forming entirely new nanostructures like carbon onions[10], double-walled carbon nanotubes[11] and hybrid carbon–BN nanotubes[12].

The structure of carbon nanotubes can be modified using electron[13–15] or ion-beam[16,17] irradiation. High irradiation doses eventually lead to the amorphization of the structure[18]. The only study performed so far on SWNT bundles has shown that the tubes can coalesce under energetic, 1.5-MeV electron irradiation at 800 °C with

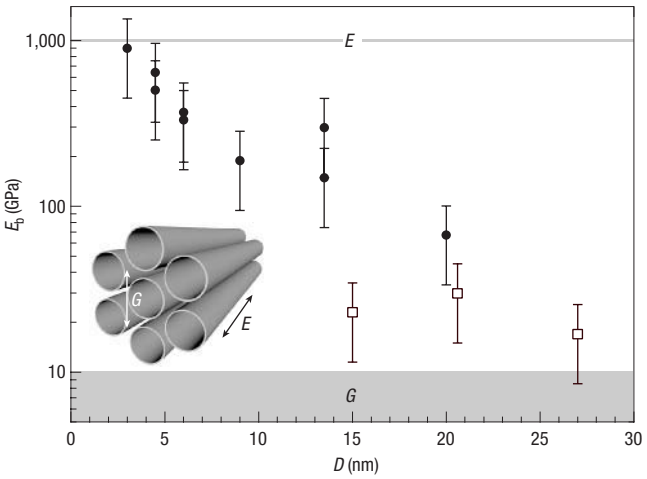

Figure 1 Dependence of the bending modulus E_b of twelve carbon nanotube ropes on the tube diameter *D*. The bending modulus of thin tubes corresponds more closely to the Young's modulus (*E*). For thicker tubes, the bending modulus decreases due to sliding between the tubes and approaches the value of the shear modulus (*G*). *E* can be reached by forming irradiation-induced crosslinks between the tubes. The open squares indicate the initial E_b for the three ropes that were irradiated and used in this study. The inset represents a simplified sketch of a carbon nanotube rope. The shear modulus (*G*) describes the resistance to intertube sliding, and the Young's modulus (*E*) describes the resistance to longitudinal stretching.

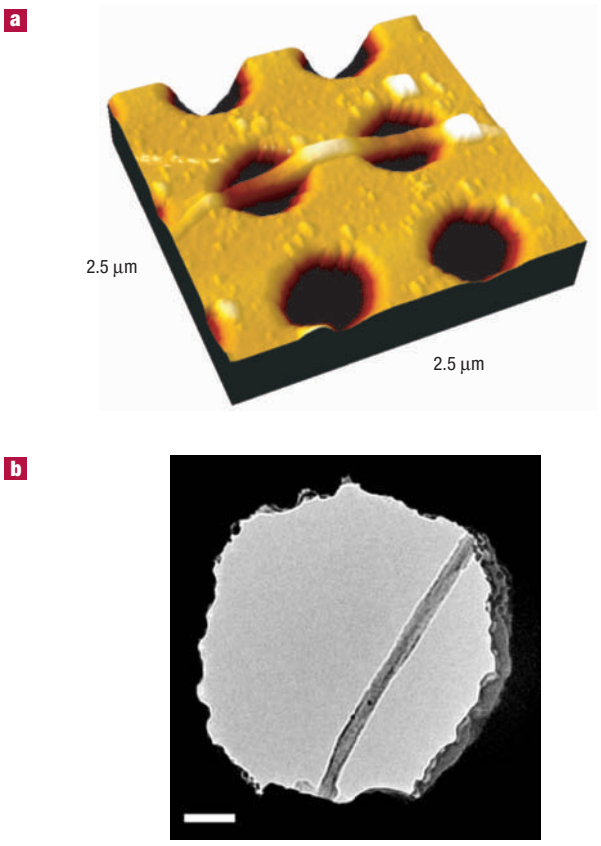

Figure 2 Dependence of E_b of carbon nanotube ropes on the irradiation dose. AFM measurements, TEM observation and irradiation were carried out on the same nanotube rope. **a**, Three-dimensional rendering based on the AFM image of a carbon nanotube rope spanning two holes. Measurements were performed on the hole on the right side. **b**, TEM image of the same nanotube (scale bar 100 nm). The rope appears to be broader on the AFM image because of convolution with the tip shape. **c**, Behaviour of E_b of different carbon nanotube ropes as a function of received dose for two incident electron energies. For 200 keV, the bending modulus increases on short exposures, due to crosslinking and degrades at higher exposures because of structural damage. The rope irradiated with 80-keV electrons shows a much stronger and sharper increase of the bending modulus. Lines are given for clarity. The inset shows a sketch of crosslinked nanotubes in the rope.

two or more tubes joining into a new tube with a bigger diameter[14]. Similar conditions can also lead to junction formation between single, isolated tubes in the area of their contact[15], though with apparent degradation of structure outside the contact area[19]. Electrical coupling between individual tubes comprising a bundle can also be enhanced by introducing defects using Ar^+ ion irradiation[16]. Pitch-based carbon fibres with typical diameters in the 100-µm range can also be modified by ion-beam irradiation. Exposure to 170-keV electrons increases their resistance to fracture[20], whereas high-energy (175 MeV) argon ions can decrease their diameter and both increase or decrease their tensile strength and Young's modulus by up to 70%, depending on the type of the fibre[21].

A charged particle beam has two major effects, depending on the energy transfer from the incoming particles to the target. For small energy transfers (of the order of several electron volts), only electronic excitation of valence electrons occurs. Excited states can lead to local chemical modifications by atomic-bonding instabilities and rearrangement (radiolysis). Above a certain threshold, incoming particles have a sufficiently high kinetic energy to displace atoms from the lattice by direct elastic collisions with the nuclei. The primary mechanism for damaging carbon nanotubes is along the path of direct knock-on collisions. Previous studies[22] have shown that the threshold energy for elastic carbon displacement in isolated SWNTs is 86 keV. Electrons below this energy can still lead to the formation of interstitials. The threshold value can also be smaller near defects, due to a lower coordination number[23].

To ascertain the most efficient mechanism of producing crosslinks, we have used electron energies both below (80 keV) and above (200 keV) the displacement threshold in isolated SWNTs. SWNT bundles grown by arc discharge and purified using an H_2O_2/HCl mixture were dispersed in ethanol and deposited on a micro-fabricated, free-standing and perforated Si_3N_4 thin membrane before electron irradiation in the transmission electron microscope (TEM). Such a set-up allows elastic

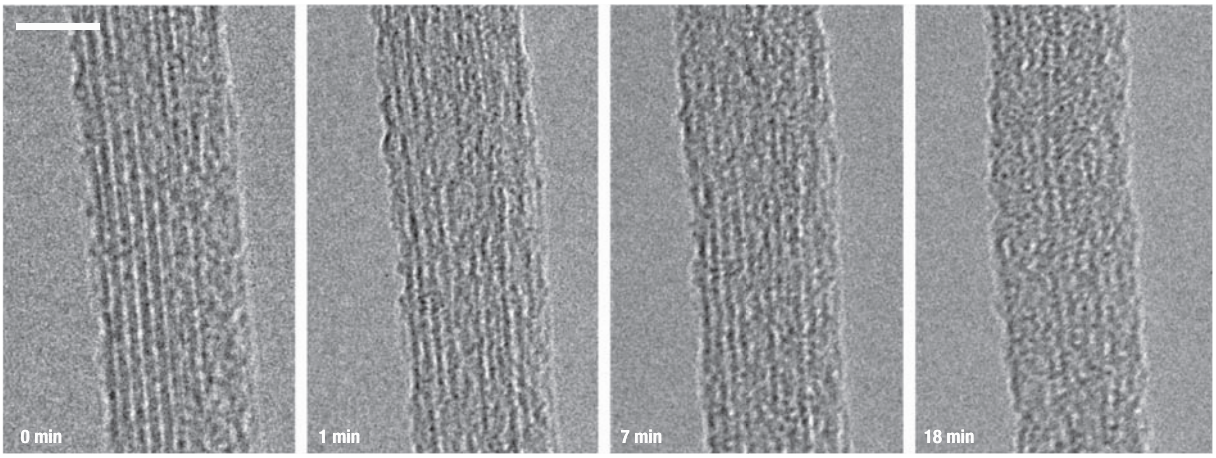

Figure 3 Evolution of the morphology of a carbon nanotube rope under electron-beam irradiation. The acceleration voltage was 200 kV with a flux of 1.35×10^{19} e cm^{-2} s^{-1}. Exposures corresponding to times indicated on the images are (from left to right) 0, 8.1×10^{20}, 60×10^{20} and 150×10^{20} e cm^{-2}. The scale bar is 10 nm.

measurements, TEM observation and irradiation to be performed on the same, isolated SWNT bundle (Fig. 2a,b). Acid purification and sonication were kept at minimum to avoid damaging the tubes. Ropes were irradiated at room temperature using an electron beam with the flux of 1.35×10^{19} e cm^{-2} s^{-2}, which corresponds to a current density of 2 A cm^{-2} that was maintained constant during the irradiation experiment. After each exposure to the electron beam, the irradiated nanotube bundle was located by means of an atomic force microscope (AFM). The bending modulus of the carbon nanotube rope was measured using an AFM tip by vertically deflecting the suspended part of the tube[2]. Using this method, a correlation between structural order and elastic properties of multiwalled carbon nanotubes (MWNTs) has been demonstrated, showing that the bending modulus of MWNTs decreases as the disorder in their structure increases[24].

Specific to SWNT bundles is their low shear modulus, which has to be taken into account when calculating the bending modulus. The deflection of the nanotube bundle over a perforation follows the expression:

$$\delta = \frac{FL^3}{192EI} + f_s \frac{FL}{4GA} = \frac{FL^3}{192E_bI} \qquad (1)$$

with L the suspended length, E the Young's modulus, f_s a constant numerical factor determined by the geometry and equal to 10/9, G the shear modulus, I the second moment of the tube's cross-section and E_b the effective bending modulus[25]. In a simpler form, the effective bending modulus of a cylindrical bar can be written in the following way:

$$\frac{1}{E_b} = \frac{1}{E} + \frac{10}{3}\frac{D^2}{L^2}\frac{1}{G} \qquad (2)$$

where D is the rope diameter. In as-produced ropes, E remains constant, reflecting the single-tube stiffness; G is found to decrease slightly when the rope diameter increases.

Figure 2c shows the variation of the bending modulus of single bundles for increasing exposure to 200 and 80 keV electrons, respectively. In the case of a 200-keV beam, the change of the bending modulus is non-monotonic, highlighting the competition of two different mechanisms during the irradiation process. For low doses, a substantial increase of E_b is observed, suggesting that crosslinking effectively occurred, leading to an increase in G, whereas the irradiation damage remains limited so that the initially high E is maintained. For long irradiation times, decrease of E_b was observed. The reason for this decrease can be seen in the 'snapshots' of TEM images (Fig. 3) taken just before each of the bending-modulus measurements. For higher doses, the well-ordered structure of tubes within the bundle disappears due to extended irradiation damage and the Young's modulus gradually decreases. The beam shrinks and becomes amorphous. The bending modulus we found at this stage was in agreement with results of nanoindentation experiments performed on irradiated amorphous carbon films[26].

At 80 keV, electrons have been shown not to damage isolated single-walled carbon nanotubes[22]. In the case of bundles, these electrons have enough energy to lead to the formation of mobile interstitial atoms in the confined space between neighbouring tubes. We have found a huge increase of the bending modulus, by a factor of thirty—up to 70% of the value for isolated SWNTs. Such a huge increase suggests that the links appearing between the tubes could be covalent bonds between carbon atoms. Local strain caused by crosslinking decreases the threshold value for knock-on displacements. As a consequence, damage to the structure starts to accumulate and the bending modulus eventually decreases. Irradiation above the threshold energy of 86 keV is less effective, because intra- and intertube bonds are destroyed by knock-on collisions as irradiation proceeds. It is interesting to note that the highest reported improvement of the static modulus of graphite by neutron irradiation was only by a factor of three[27].

Tubes inside ropes are separated by 0.34 nm, twice the van der Waals radius of carbon atoms. Such a large distance cannot be bridged by a single sp^3 bond, so the nature of crosslinks between the nanotubes needs to be further investigated. First-principles modelling of defects in irradiated graphite has shown that divacancies and interstitials (in a sheared lattice) can form bridges between adjacent atomic planes[28].

Molecular dynamics simulations of energetic Ar^+ ion impacts on SWNT bundles have shown that neighbouring tubes can be bridged by covalent carbon–carbon bonds mediated by carbon atom recoils[29]. Carbon atoms that end up as mobile interstitials after having been knocked-out from tubes or coming from residues of the purification procedure are the primary candidates for these intertubular links.

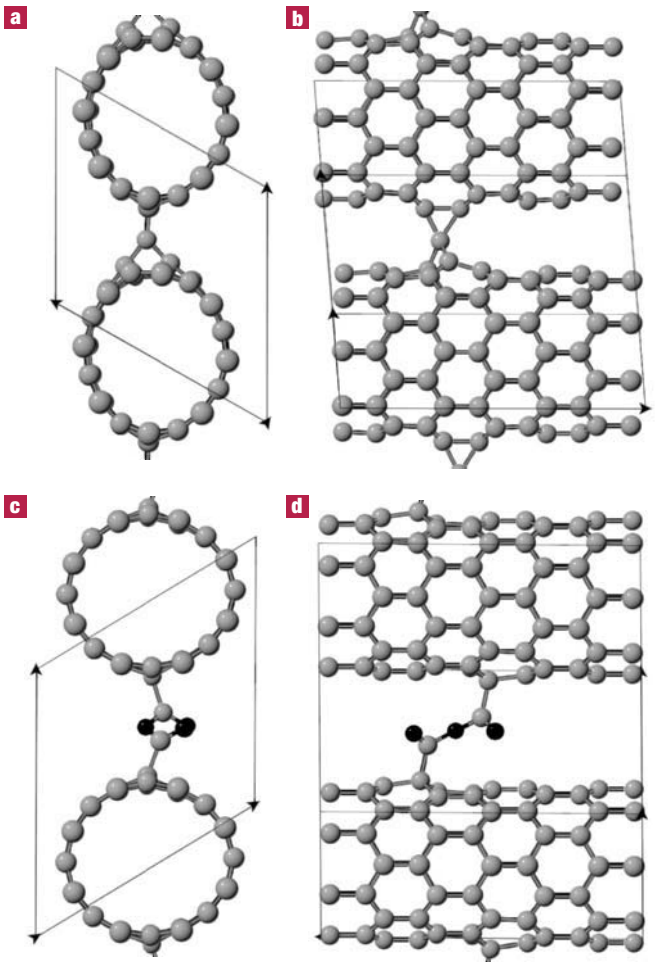

Figure 4 Atomic models based on DFT calculations of two different kinds of bridges formed between neighbouring carbon nanotubes. a,**b**, Frontal (**a**) and side view (**b**) of a bridge involving carbon atoms formed through a fourfold coordinated interstitial carbon atom. **c**,**d**, Frontal (**c**) and side view (**d**) of crosslink fromed in an electron-beam-induced chemical reaction between carboxyl functional groups attached to neighbouring nanotubes. Oxygen atoms are shown in black.

Carbon atoms close to defect sites can be moved to interstitial positions even during collisions with 80-keV electrons. Other species like oxygen and nitrogen molecules adsorbed from air or hydroxyl and carboxyl groups resulting from the acid purification treatment[30] could participate in crosslinking.

We have investigated the possibility of crosslink formation using a model based on a density-functional theory (DFT). The plane-wave pseudopotential DFT calculations were carried out with the CASTEP code[31], using the PBE (Perdew–Burke–Ernzerhof) gradient corrected exchange-correlation functional[32]. One possibility is a bridge shown on Fig. 4a,b, where the connection to the two nanotubes is formed by a fourfold coordinated interstitial carbon atom. On top, the adatom is on a bond, forming a triangle with angles of 60 ± 3 degrees, and sides of 1.5–1.6 Å. On the bottom, one of the bonds in the hexagonal network was broken, and the resulting two new bonds are 1.5 ± 0.02 Å long, with an angle of 88 degrees between them. Interstitial carbon atoms formed during irradiation are mobile at room temperature. They could move in the space between the nanotubes before getting into a position suitable for stable bridge formation. Two carboxyl groups on neighbouring nanotubes can also form a stable crosslink. In the carboxyl bridge shown on Fig. 4c,d, the C–C bonds to the tubes are 1.53 ± 0.01 Å long, the C=O bonds are 1.2 ± 0.01 Å long, and the C–O–C bond lengths are 1.38 ± 0.01 Å with an angle of 122 degrees between them. Single carboxyl and hydroxyl groups from which hydrogen would be removed by irradiation did not form crosslinks. The crosslinking through functional groups is therefore much less probable, as it requires the presence of two identical groups close to each other on opposing nanotubes (Fig. 4d).

We computed the shear modulus of a pair of nanotubes connected with the above bridges, by adjusting the unit cell so as to displace the two tubes slightly along their common axis, and reoptimizing the internal coordinates. For both bridges, we estimate a shear modulus of about 200 GPa at an interlink density of 0.8 nm^{-1}. To realise the experimentally observed increase in shear modulus, the interlink density would have to be three times this, which is not implausible, given that a tube can form links with any one of six neighbours in a nanotube bundle. On the other hand, such a relatively high interlink density makes crosslinking through functional groups even less probable, as it would require a rather high degree of nanotube functionalization in the confined intertube area.

In conclusion, we have used a combination of AFM and TEM techniques on the same isolated carbon nanotube bundle to quantify radiation-induced morphological and mechanical property changes. Measurements of the bending modulus as a function of exposure to the electron-beam gave new insights into the dynamics and mechanisms of radiation-induced modifications of carbon nanotubes. At low doses the appearance of crosslinking was observed, with tubes becoming amorphous at longer exposures.

Crosslinking is most probably not due to a local change in atom hybridization only, because of a prohibitively large intertube distance. Theoretical modelling has shown that crosslinks can form with the participation of interstitial carbon atoms created by irradiation, or by a radiation-induced chemical reaction between carboxyl groups, which requires the simultaneous presence of two chemical groups on opposing nanotubes and is therefore much less probable.

These observations together suggest that electron irradiation could be used for connecting carbon nanotubes together. This method offers a new and exciting opportunity of building larger-scale structures composed of strongly connected carbon nanotubes, using dedicated cathode-ray sources.

Received 14 October 2003; accepted 19 January 2004; published 15 February 2004.

References

1. Iijima, S. Helical microtubules of graphitic carbon. *Nature* **354,** 56–58 (1991).
2. Salvetat, J.-P. *et al.* Elastic and shear moduli of single-walled carbon nanotube ropes. *Phys. Rev. Lett.* **82,** 944–947 (1999).
3. Lu, J. P. Elastic properties of carbon nanotubes and nanoropes. *Phys. Rev. Lett.* **79,** 1297–1300 (1997).
4. Thess, A. *et al.* Crystalline ropes of metallic carbon nanotubes. *Science* **273,** 483–487 (1996).
5. Vigolo, B. *et al.* Macroscopic fibers and ribbons of oriented carbon nanotubes. *Science* **290,** 1331–1334 (2000).
6. Dalton, A. B. *et al.* Super-tough carbon-nanotube fibres. *Nature* **423,** 703 (2003).
7. Zhu, H. W. *et al.* Direct synthesis of long single-walled carbon nanotube strands. *Science* **296,** 884–886 (2002).
8. Banhart, F. Irradiation effects in carbon nanostructures. *Rep. Prog. Phys.* **62,** 1181–1222 (1999).
9. Banhart, F. & Ajayan, P. M. Carbon onions as nanoscopic pressure cells for diamond formation. *Nature* **382,** 433–435 (1996).
10. Ugarte, D. Curling and closure of graphitic networks under electron-beam irradiation. *Nature* **359,** 707–709 (1992).
11. Smith, B. W., Monthioux, M. & Luzzi, D. E. Encapsulated C60 in carbon nanotubes. *Nature* **396,** 323–324 (1998).
12. Mickelson, W., Aloni, S., Han, W.-Q., Cumings, J. & Zettl, A. Packing C60 in boron nitride nanotubes. *Science* **300,** 467–469 (2003).
13. Ajayan, P. M., Ravikumar, V. & Charlier, J.-C. Surface reconstructions and dimensional changes in single-walled carbon nanotubes. *Phys. Rev. Lett.* **81,** 1437–1440 (1998).
14. Terrones, M., Terrones, H., Banhart, F., Charlier, J.-C. & Ajayan, P. M. Coalescence of single-walled carbon nanotubes. *Science* **288,** 1226–1229 (2000).
15. Terrones, M. *et al.* Molecular junctions by joining single-walled carbon nanotubes. *Phys. Rev. Lett.* **89,** 075505 (2002).
16. Stahl, H., Appenzeller, J., Martel, R., Avouris, Ph. & Lengeler, B. Intertube coupling in ropes of single-wall carbon nanotubes. *Phys. Rev. Lett.* **85,** 5186 (2000).

17. Krasheninnikov, A. V., Nordlund, K., Sirviö, M., Salonen, E. & Keinonen, J. Formation of ion-irradiation-induced atomic-scale defects on walls of carbon nanotubes. *Phys. Rev. B* **63,** 245405 (2001).
18. Zhang, Y. & Iijima, S. Microstructural evolution of single-walled carbon nanotubes under electron irradiation. *Phil. Mag. Lett.* **80,** 427–433 (2000).
19. Krasheninnikov, A. V., Nordlund, K., Keinonen, J. & Banhart, F. Ion-irradiation-induced welding of carbon nanotubes. *Phys. Rev. B* **66,** 245403 (2002).
20. Nishi, Y., Toriyama, T., Oguri, K., Tonegawa, A. & Takayama, K. High fracture resistance of carbon fiber treated by electron beam irradiation. *J. Mater. Res.* **16,** 1632–1635 (2001).
21. Oku, T., Kurumada, A., Kawamata, K. & Inagaki, M. Effects of argon ion irradiation on the microstructures and physical properties of carbon fibers. *J. Nucl. Mater.* **303,** 242–245 (2002).
22. Smith, B. W. & Luzzi, D. E. Electron irradiation effects in single wall carbon nanotubes. *J. App. Phys.* **90,** 3509–3515 (2001).
23. Crespi, V. H., Chopra, N. G., Cohen, M. L., Zettl, A. & Louie, S. G. Anisotropic electron-beam damage and the collapse of carbon nanotubes. *Phys. Rev. B* **54,** 5927–5931 (1996).
24. Salvetat, J.-P. *et al.* Elastic modulus of ordered and disordered multiwalled carbon nanotubes. *Adv. Mater.* **11,** 161–165 (1999).
25. Gere, J. M. & Timoshenko, S. P. *Mechanics of Materials* (PWS-Kent, Boston, USA, 1984).
26. Lee, D.-H., Lee, H., Park, B., Poker, D. B. & Riester, L. The effect of implantation temperature on the surface hardness, elastic modulus and Raman scattering in amorphous carbon. *App. Phys. Lett.* **70,** 3104–3106 (1997).
27. Goggin, P. R. & Reynolds, W. N. Elastic constants of reactor graphites. *Phil. Mag.* **16,** 317–330 (1967).
28. Telling, R. H., Ewels, C. P., El-Barbary, A. A. & Heggie, M. I. Wigner defects bridge the graphite gap. *Nature Mater.* **2,** 333–337 (2003).
29. Salonen, E., Krasheninnikov, A. V. & Nordlund, K. Ion-irradiation-induced defects in bundles of carbon nanotubes. *Nucl. Instrum. Meth. B* **193,** 603–608 (2002).
30. Hiura, H., Ebbesen, T. W. & Tanigaki, K. Opening and purification of carbon nanotubes in high yields. *Adv. Mater.* **7,** 275–276 (1995).
31. Segall, M. D. *et al.* First-principles simulation: ideas, illustrations and the CASTEP code. *J. Phys. Condens. Mat.* **14,** 2717–2744 (2002).
32. Perdew, J. P., Burke, K. & Ernzerhof, M. Generalized gradient approximation made simple. *Phys. Rev. Let.* **77,** 3865–3868 (1996).

Acknowledgements

We would like to thank the Centre Interdépartmental de Microscopie Electronique (CIME) at the EPFL for giving us access to the electron microscopes. We would also like to thank Silvija Gradečak and Guido Milanesi for training and technical assistance with the electron microscope and Simon Benjamin for cutting the substrates. Interesting discussions with David Tománek, Peter Stevens, Jean-Marc Bonard and Klaus Leifer are also very much appreciated. The work is partially supported by 'Nanoscale Science' NCCR (National Center of Competence in Research) and grant 20-61735.00 of the Swiss National Science Foundation. Computational work was carried out at the CCHPCF (Cambridge-Cranfield High Performance Computing Facility), University of Cambridge and supported by grant EC HPRN-CT-2000-00154.
Correspondence and requests for materials should be addressed to L.F.

Competing financial interests

The authors declare that they have no competing financial interests.